RSC Advances

ROYAL SOCIETY OF CHEMISTRY

www.rsc.org/advances

Vibronic Spectra for Organic Electronic Chromophores[†]

Azzam Charaf-Eddin[a,b], Thomas Cauchy[c], François-Xavier Felpin[a,d] and Denis Jacquemin*[a,d]

Received Xth XXXXXXXXXX 20XX, Accepted Xth XXXXXXXXX 20XX
First published on the web Xth XXXXXXXXXX 200X
DOI: 10.1039/b000000x

In this work, we illustrate how Time-Dependent Density Functional Theory (TD-DFT) that has become an everyday black-box tool for assessing the nature of electronic excited-states, can be used to reach accurate and throughout analysis of experimental optical spectra for a series of organic molecules recently proposed as building blocks for organic electronic devices. The results that yield insights regarding band shape and extinction coefficients are shown to provide more relevant information than the one obtained by the popular vertical approximation. Cases with several overlapping vibronic bands are also discussed. For the vast majority of treated molecules (10/11) the agreement between theoretical and experimental 0-0 energies and band topologies are really excellent, paving the way towards more refined theoretical designs of new organic electronic chromophores.

1 Introduction

To complement experimental measurements, theoretical calculations have become an increasingly popular tools for experimentalists. Without dispute, the most widely used theoretical model is Density Functional Theory (DFT), and, more specifically the extremely popular B3LYP approach.[1] While DFT is an adequate method to explore the geometry and reactivity of molecules in their electronic ground-state, the information brought by DFT for the analysis of optical spectra or photochemical events remains extremely sketchy. Indeed, DFT calculations provide molecular orbitals, but the use of the HOMO and LUMO frontier orbitals to analyze optical signatures is not an appropriate choice. Indeed, even if the electronic transitions in the near UV and visible spectra imply almost essentially the frontier molecular orbitals rather than a complex blend, the HOMO-LUMO energy gaps provide very poor approximations of the maximal absorption ($\lambda_{\max}$). This is due to the complete neglect of electronic relaxation effects that always occur. These effects, can be properly accounted for in TD-DFT,[2,3] which yields a solution of the time-dependent (TD) Schrödinger equation. TD-DFT has become more and more used by non-specialists in the last five years to help analyzing experimental spectra, and one could easily find numerous recent examples of TD-DFT applications in top-notch organic journals.[4–23] The large majority of these TD-DFT applications rely on the so-called vertical approximation: the transition energies to the lowest excited-state(s) are computed with TD-DFT on a frozen ground-state geometry. This protocol has however, several drawbacks: i) absolutely no indication on the fluorescence properties is obtained; ii) the neglect of the coupling terms between vibrational and electronic motions (vibronic effects) does not allow to predict band shapes in a consistent way; iii) vertical transition energies cannot be compared to experimental $\lambda_{\max}$ on a solid physical basis due to the neglect of both vibrational and geometry reorganization effects; and iv) the same holds for the experimental molar absorption coefficients (ε) that cannot be directly obtained from vertical calculations.

During the last decade, there has been numerous theoretical developments aiming to improve TD-DFT and this notably includes the implementation of TD-DFT forces and Hessian that give respectively access to geometry optimization and vibrational analysis at the excited state.[24–27] In turns, this allows to efficiently explore the potential energy surface of the excited states, to obtain fluorescence wavelengths and Stokes shifts as well as to rapidly account for the most important vibronic couplings. Whilst these methodologies have already found applications for “real-life” structures,[28–40] they remain often unused by the non-specialists. In the present work, we illustrate the interest of these new approaches taking as working examples several structures that have appeared in organic chemistry journals. More specifically, the molecules studied here have been selected in contributions devoted to the design of molecules with potential impact in organic electronic de-

---

[†] Electronic Supplementary Information (ESI) available: Additional spectra and molecules, Cartesian coordinates, Movies of the vibrational modes. See DOI: 10.1039/b000000x/

[a] *Chimie Et Interdisciplinarité, Synthèse, Analyse, Modélisation (CEISAM), UMR CNRS no. 6230, BP 92208, Université de Nantes, 2, Rue de la Houssinière, 44322 Nantes, Cedex 3, France. E-mail: denis.jacquemin@univ-nantes.fr.*

[b] *Present address: Centre Interdisciplinaire de Nanoscience de Marseille (CINam), UMR CNRS no 7325, Aix Marseille Université, Campus de Luminy, Case 913, 13288 Marseille Cedex 9, France.*

[c] *Laboratoire MOLTECH-Anjou - UMR CNRS 6200, Université d'Angers, 2 Blvd Lavoisier, 49045 Angers, France.*

[d] *Institut Universitaire de France, 103, blvd Saint-Michel, F-75005 Paris Cedex 05, France.*

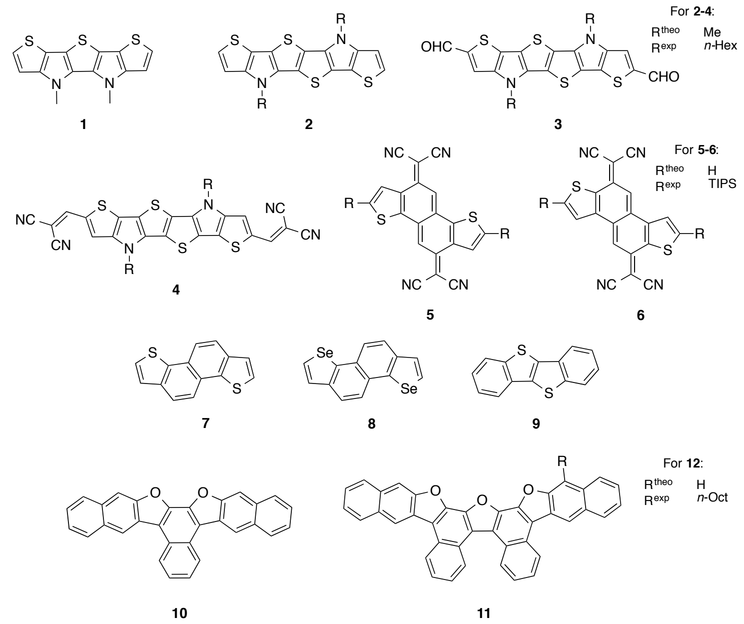

Fig. 1 Representation of the set of molecules investigated in this work.

vices. The accurate simulations of their optical signatures is therefore of prime importance. These compounds are represented in Figure 1. We redirect the interested reader to the original works (**1**[41], **2**–**4**,[42] **5**–**6**,[43] **7**–**9**,[44] and **10**–**11**[45]) for synthetic and experimental details, that are clearly beyond our scope here.

2 Computational Details

All calculations have been performed with the latest version of the Gaussian 09 program package,[52] applying a tight self-consistent field convergence criterion $(10^{-9}-10^{-10})$ a.u. and a strict optimization threshold $(10^{-5}$ a.u. on average forces). The same DFT integration grid, namely the *ultrafine* pruned (99,590) grid, was systematically used. Indeed, the potential energy surfaces of the excited-states tend to be softer than their ground-state counterparts, and improved numerical accuracy is welcome to avoid possible instabilities. We have optimized both the ground and excited state geometries and determined their vibrational patterns systematically using DFT and TD-DFT, respectively. Following Ref. 51, we have used the 6-31+G(d) atomic basis set throughout but corrected our 0-0 energies for basis set errors using single-point 6-311++G(2df,2p) calculations. This yields converged data for low-lying excited-states in organic molecules.[51] We do not intend to discuss what is the most appropriate exchange-correlation functional here, a topic covered in details elsewhere,[53] and we have therefore used Truhlar's M06 global hybrid throughout the text,[54,55] as this hybrid often works nicely for organic compounds. In this work, we have modeled solvent effects through an implicit solvation approach, namely the Polarizable Continuum Model (PCM).[46] While for ground-state properties, the use of PCM is rather straightforward, PCM-TD-DFT calculations should be made more carefully. Indeed, there exist two different PCM regimes for excited-states: the *equilibrium* (eq) and *non-equilibrium* (neq) limits.[46] In the former, the solvent has time to fully adapt to the new state of the chomophore and this approximation is adequate for slow phenomena (e.g., optimizing the geometry of the excited-states). In the latter, only the electrons of the solvent have time to react to the change of states of the solute, a limit suited for fast phenomena (e.g., vertical absorption and emission). For assessing the polarization of the cavity in the excited-states, there exist several PCM schemes: linear-response (LR),[47,48] corrected linear response (cLR)[49] and state specific (SS).[50] To make the long story short, the traditional LR approach is suited for absorption spectra and for optimizing excited-state structures but cannot be rigorously applied to compute both emission and 0-0 energies of solvated species. We have therefore used the cLR scheme here to compute all excited-state energies. We redirect the interest readers to a recent contribution for a complete discussion of the computation of cLR 0-0 energies.[51]

Vibrationally resolved spectra within the harmonic approximation were computed using the FCclasses program (FC).[30,56,57] The reported spectra were simulated using a convoluting Gaussian function presenting a half width at half maximum (HWHM) that was adjusted to allow direct comparisons with experiments (typical value: 0.08 eV). A maximal number of 25 overtones for each mode and 20 combination bands on each pair of modes were included in the calculation. The maximum number of integrals to be computed for each class was first set to 10^6. In the cases where convergence of the FC factor [≥ 0.9] could not be achieved with this number of integrals, a larger value (up to 10^{12}) was used so to pass the 0.9 limit.

3 Results

3.1 Molecule 1

Let us start with the nitrogen-bridged terthiophene **1** proposed by Mitsudo and coworkers.[41] A comparison between theoretical and experimental band shapes is shown in Figure 2. The computed positions of the peaks are 372, 354 and 337 nm. This fits well the experimental data of 354, 339 and 320(sh) nm but for a nearly constant offset of ca. 17 nm.[58] Probably more impressive is the fact the log(ε) computed for the two first peaks are 4.70 and 4.74, very close to the experimental data of 4.62 (for both peaks), nicely illustrating the accuracy of the vibronic calculations. For the records, as the absorption between 380 to 260 nm is due to only one electronic excitation, the vertical TD-DFT approximation level would have led a single band at 357 nm with an oscillator strength of 0.9, and would have been much less relevant.[59]

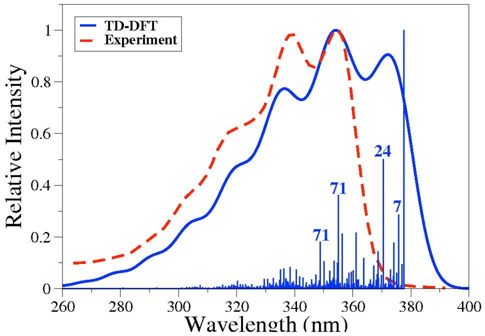

Fig. 2 Comparison between experimental (red) and theoretical (blue) band shapes for the absorption spectra of **1** in dichloromethane. Intensities have been normalized to 1 in both cases, but no offset was applied on the energy scale. Experimental spectra adapted, with permission from, Mitsudo *et al. Org. Lett.* **14** (2012) 2702–2705, Copyright 2012 American Chemical Society.

As can be seen in Figure 2, the agreement between theoretical and experimental band shapes is very good, though theory slightly overshoots the relative intensities of the second and third bands, the errors being ca. 10%, which is the expected error range for relative vibronic intensities.[60] More importantly, the stick spectra shown in Figure 2 allows to determine the vibrational modes (in the excited-state here as we consider absorption), significantly contributing to the specific band shape of the system. Here, mode 71 is particularly important. This mode, that can be found in the Supporting Information (SI), corresponds to the stretching at 1678 cm^{-1} of the C-C bond of the central thiophene connecting the two pyrroles (see Figure 1). This suggests, that the central pattern of this chomophore is responsible for the band shapes, and that substitution of the external thiophene would only slightly affect this specific topology.

3.2 Molecules 2–4

Let us now continue with rather similar structures but bearing substituents on the sides, as well as presenting a central bithiophene unit, namely, dyes **2**–**4** of Bäuerle and collaborators (see Figure 1): the position, intensity and shape of both absorption and emission bands being significantly dependent on the side groups.[42]. A comparison between theoretical and experimental data can be found in Figure 3, and the agreement is obvious at first glance. Theory restores the bathochromic shifts undergone upon substitution for both absorption and emission and accurately reproduces the relative intensities related to the two phenomena. For absorption, the measured $\varepsilon_{\max}$ ratio are 1.0:1.8:3.1 for **2**:**3**:**4** whereas the corresponding TD-DFT values extracted from our vibronic calculations are 1.0:1.9:3.4. This is a much better match experiment than the one provided by bluntly selecting the oscillator strengths from standard vertical calculations that would lead a 1.0:1.5:2.2 ranking.

The topologies of the absorption bands are also nicely reproduced with a very clear vibronic progression for the absorption of **2** (the only one not quantitatively reproduced), a very intense shoulder for **3** and a shoulder with a ca. half intensity compared to the main peak for **4**. For emission, not only are the theoretical shapes correct, but also their evolution with respect to absorption. Indeed, the emission band presents a less marked vibronic progression for **2** and less intense shoulders compared to absorption for the two substituted dyes and these evolutions are restored by theory. In Figure 4 we report the density difference plots for the three compounds that allow to investigate the nature of the excited-states on a more qualitative basis. As can be seen the states are delocalized and the cyano/aldehyde groups are mostly in red indicating that, as expected, these moieties act as electron acceptors. Therefore in **3** and **4** there is a partial charge-transfer from the core to the extremities, but this effect is far from being exclusive or vastly dominating. This conclusion of moderate charge-transfer therefore mitigates the qualitative conclusion obtained on the sole basis of the topology of the frontier orbitals.[42] The integration of the density differences gives access to the amount of transferred charges,[61,62] that was found to be smaller in **2** (0.39 *e*) than in **3** (0.46 *e*) and **4** (0.45 *e*).

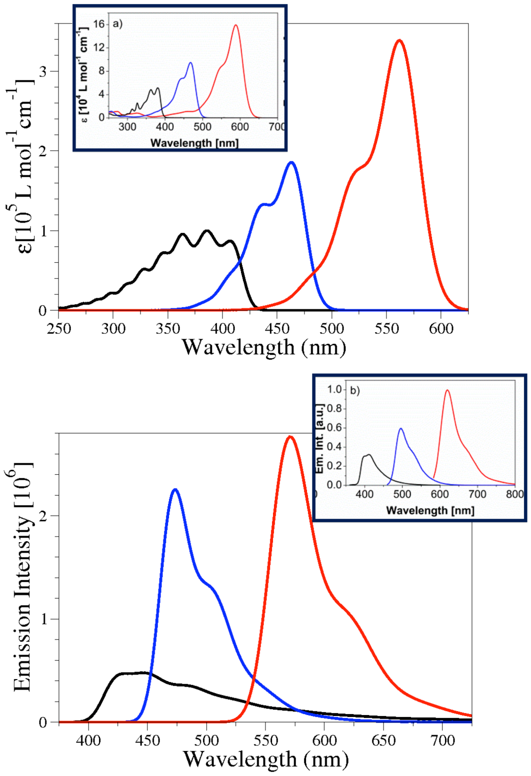

Fig. 3 Comparison between experimental (insets) and theoretical band shapes for the absorption (top) and fluorescence (bottom) spectra of **2** (black), **3** (blue) and **4** (red), in dichloromethane. No offset nor normalization was applied to the theoretical data. Experimental spectra adapted, with permission from, Wetzel *et al.* *Org. Lett.* **16** (2014) 362–365, Copyright 2014 American Chemical Society.

3.3 Molecules 5–6

We have also modeled the spectra of dithiophene-fused tetracyanonaphthoquinodimethanes, **5** and **6**, two regioisomers (α and β respectively) proposed by Yanai and coworkers.[43] We have replaced the large TIPS groups by hydrogen atoms to lighten the computational burdern, but experimentally, the nature of the substituents (R in Figure 1) has only a small impact on the absorption spectra.[43] Theoretical and experimental graphs are compared in Figure 5 and it is again obvious that our TD-DFT protocol is successful, as it provides accurate relative wavelengths and intensities as well as correct band shapes for both dyes. Nevertheless, the absolute ε are overestimated by theory, and the difference of intensity between the most intense band of **5** and **6** is slightly underrated. The stick spectra for the two dyes are available in the ESI as well as the movies of the key vibrational mode (n^o 79) that is centered on the naphto core and is therefore similar for the two dyes. We note that vertical calculations that provide the correct bathochromic displacement between the α (**5**) and β (**6**) derivatives, incorrectly predict the ordering of the intensities: the associated oscillators strengths are 1.10 and 1.26, respectively (see central panel in Figure 5).

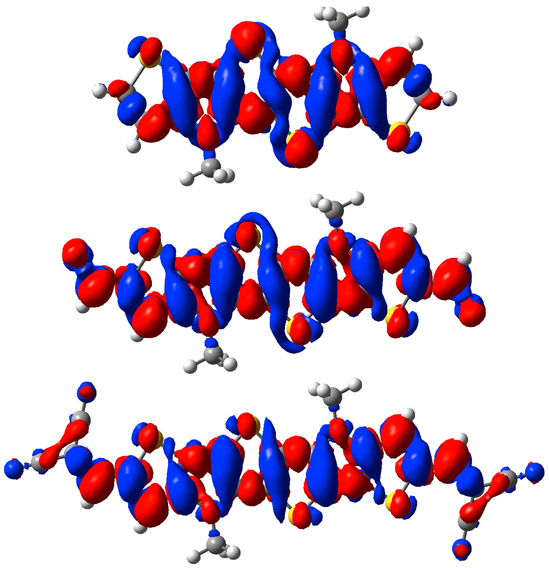

Fig. 4 Density difference plots for (from top to bottom): **2**, **3** and **4**. The blue (red) regions indicate decrease (increase) of the electronic density upon absorption of light.

3.4 Molecules 7–9

These three small chrompohores, that have been fully characterized experimentally in 2010,[44] constitute an interesting series due to the presence of several transitions that are close on the energetic scale, leading to overlapping of bands, each having its own shape. In Figure 6, the vibronic band shapes of the first four electronically excited states of **7** are shown, together with their addition that can be compared to the experimental spectrum. Our calculations indicate that the second excited-state yields a completely negligible contribution, that the first excited-state provides a relatively weak but broad and structured absorption in the 320–360 nm domain, whereas the shape of the most intense experimental band can be due to the combination of the third and fourth electronically excited states. It is the latter state that “transforms” the marked second vibronic peak of the third state to a shoulder (see top panel of Figure 6). We note nevertheless that theory misses some absorption at ca. 300 nm and overestimates the intensity of the absorption at longer wavelengths.

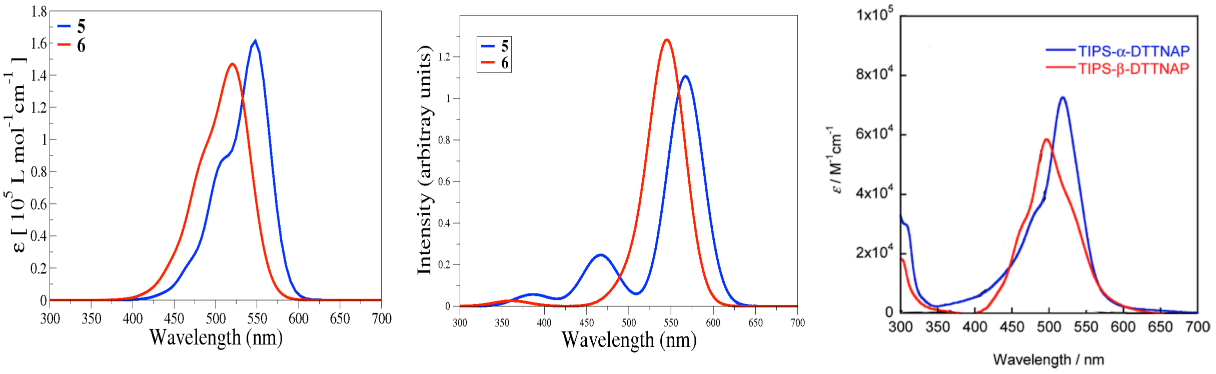

Fig. 5 Comparison between theoretical (left: vibronic; center: vertical) and experimental (right) absorption spectra of **5** (blue) and **6** (red) in dichloromethane. No offset nor normalization was applied to the theoretical data. Experimental spectra adapted, with permission from, Yanai *et al. Org. Lett.* **16** (2014) 240–243, Copyright 2014 American Chemical Society.

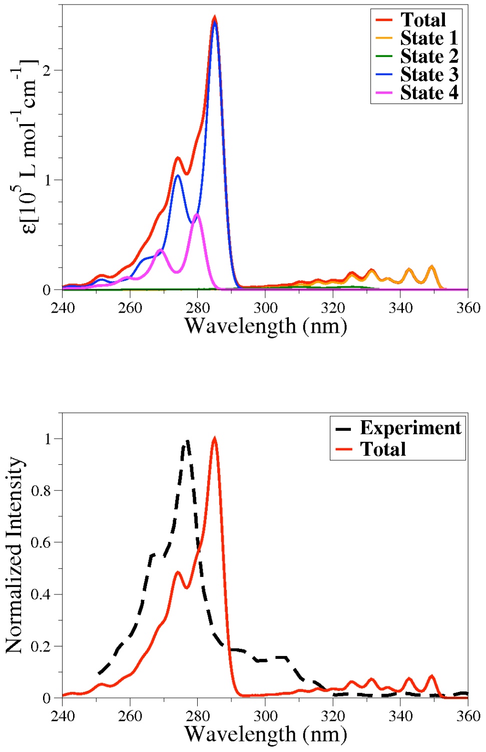

Fig. 6 Top: vibrationally resolved spectra computed for the first four states of **7**. Bottom: comparison between computed and measured absorption spectra, no offset applied but intensities normalized to allow straightforward comparisons of relative heights. The solvent is dichloromethane. Experimental spectra adapted, with permission from, Shinamura *et al. J. Org. Chem.* **75** (2010) 1228–1234, Copyright 2010 American Chemical Society.

For molecule **8** (Figure 7), the situation is similar but there are only two excited-states significantly contributing to the final band shapes, the first and the third states, respectively leading to absorption in the 320–370 and 260–310 nm domains. For **8**, TD-DFT foresees no significant overlap between these individual contributions. As for its sulfur counterpart, both absolute and relative intensities of the long-wavelength absorption are overshot by TD-DFT for the seleno **8**. Comparisons of **7** and **8** indicates that the replacement of sulfur atoms by selenium atoms induces, despite apparently similar band topologies, a variation of the nature of the individual components.

9 is an example in which TD-DFT becomes less efficient. Indeed, one clearly notices on the bottom panel of Figure 7 the presence of two bands above 280 nm, a fact correctly restored by theory but the details of the spectrum (both absolute and relative intensities of the two peaks, shape of both bands, etc.) are not satisfying. Such outcome can be related either to the selected exchange-correlation functional (M06), to the application of the harmonic vibrational approximation or to the specific effects (e.g., aggregation) not accounted for in the calculation.

3.5 Molecules 10–11

Finally, we have tackled two large butterfly-like π-conjugated systems proposed in 2014,[45] to confirm that the accuracy obtained for the rather compact dyes is maintained for more extended architectures. The results are displayed in Figure 8 and once again, TD-DFT provides good insights, reproducing the **10**→**11** bathochromic shift of first band, as well as the overlapping position of the second (third) band of **11** and the first (second) of **10**. The overall vibronic progression is also reasonably reproduced in both cases. Eventually, additional examples for three fused-thiophene derivatives can be found in the ESI.

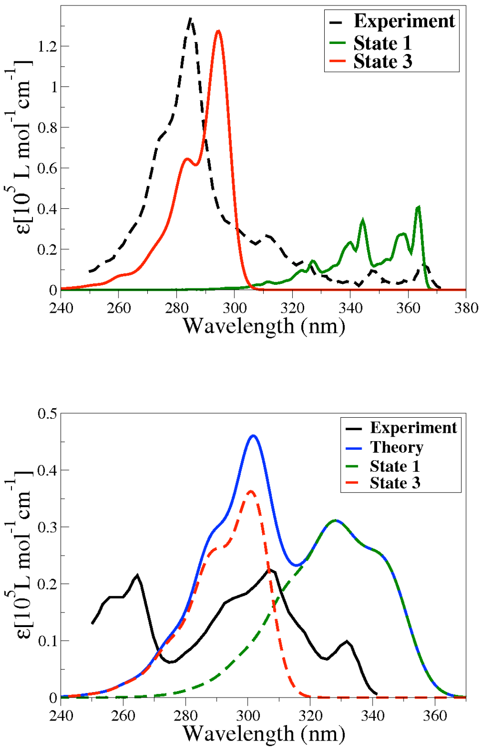

Fig. 7 Top: Comparison between experimental and theoretical (no offset no normalization) for molecule **8**. Bottom: Comparison between experimental and theoretical (no offset no normalization) for molecule **9**. All results in dicholoromethane. Experimental spectra adapted, with permission from, Shinamura *et al. J. Org. Chem.* **75** (2010) 1228–1234, Copyright 2010 American Chemical Society.

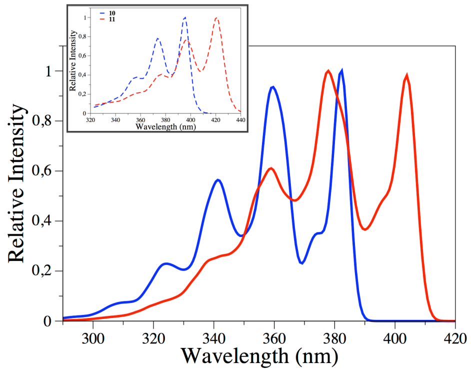

Fig. 8 Comparison between experimental (inset) and theoretical band shapes for the absorption spectra of **10** (blue) and **11** (red) in tetrahydrofuran. Experimental spectra adapted, with permission from, Nakanishi *et al. J. Org. Chem.* **79** (2014) 2625–2631, Copyright 2014 American Chemical Society.

4 Conclusions

In this contribution, we have applied state-of-the-art TD-DFT approaches to mimic the spectral features (both absorption and emission spectra) of a series of conjugated structures recently proposed for applications in organic electronics. Despite the approximation inherent to the use of TD-DFT, the match with experimental data is generally excellent, only one out of 11 cases leading to a poor agreement. This performance holds not only for spectroscopic properties (position of absorption and emission bands, molar extinction coefficient and band shape) but also for their evolution with chemical modifications (regioisomers, substitution, etc.). Our vibrationnally-resolved electronic spectra allowed a refined analysis of the experimental data (e.g. understanding overlapping bands, identifying key vibrational modes, etc.) subsequently paving the way towards a more rational and efficient design of new molecules with specific spectral signatures.

This work also illustrates the limits of the usually-applied vertical TD-DFT approximation. For instance, we have found several examples in which the relative experimental ε cannot be understood by investigating the relative (vertical) oscillator strengths even in structurally similar chromophores. It is therefore our hope that this work will participate in the stimulation of the use a more "modern" TD-DFT approaches outside the theoretical community.

Acknowledgment

A.C.E. thanks the European Research Council (ERC, Marches no°278845) and the Région des Pays de la Loire for his post-doc grant. D.J. also acknowledges both the ERC for the starting grant (Marches no°278845) and the Région des Pays de la Loire Loire for the *recrutement sur poste stratégique*. Allocations of computation time from the GENCI-CINES/IDRIS (c2014085117), the C CIPL (*Centre de Calcul Intensif des Pays de Loire*), and the CEISAM's Troy cluster are gratefully acknowledged.

References

1 A. D. Becke, *J. Chem. Phys.*, 1993, **98**, 5648–5652.
2 E. Runge and E. K. U. Gross, *Phys. Rev. Lett.*, 1984, **52**, 997–1000.
3 M. E. Casida, in *Time-Dependent Density-Functional Response Theory for Molecules*, ed. D. P. Chong, World Scientific, Singapore, 1995, vol. 1, pp. 155–192.
4 M. Zhang, Y. Zhu, G. Zhan, P. Shu, R. Sa, L. Lei, M. Xiang, Y. Xue, Z. Luo, Q. Wan, G. Yao and Y. Zhang, *Org. Lett.*, 2013, **15**, 3094–3097.
5 E. Procházková, L. Čechová, Z. Janeba and M. Dračínský, *J. Org. Chem.*, 2013, **78**, 10121–10133.
6 W. C. W. Leu and C. S. Hartley, *Org. Lett.*, 2013, **15**, 3762–3765.
7 P.-A. Bouit, L. Infantes, J. Calbo, R. Viruela, E. Ortí, J. L. Delgado and N. Martín, *Org. Lett.*, 2013, **15**, 4166–4169.

8 K. Takata, M. Iwatsuki, T. Yamamoto, T. Shirahata, K. Nonaka, R. Masuma, Y. Hayakawa, H. Hanaki, Y. Kobayashi, G. A. Petersson, S. Omura and K. Shiomi, *Org. Lett.*, 2013, **15**, 4678–4681.

9 R. C. Jones, K. Herasymchuk, T. Mahdi, A. Petrov, S. Resanovic, D. G. Vaughan, A. J. Lough, J. W. Quail, B. D. Koivisto, R. S. Wylie and R. A. Gossage, *Org. Biomol. Chem.*, 2013, **11**, 3484–3493.

10 V. F. Pais, M. Lineros, R. López-Rodríguez, H. S. El-Sheshtawy, R. Fernández, J. M. Lassaletta, A. Ros and U. Pischel, *J. Org. Chem.*, 2013, **78**, 7949–7961.

11 T. Nishinaga, T. Kageyama, M. Koizumi, K. Ando, M. Takase and M. Iyoda, *J. Org. Chem.*, 2013, **78**, 9205–9213.

12 L. Zilbershtein-Shklanovsky, M. Weitman, D. T. Major and B. Fischer, *J. Org. Chem.*, 2013, **78**, 11999–12008.

13 L. Long, L. Zhou, L. Wang, S. Meng, A. Gong, F. Du and C. Zhang, *Org. Biomol. Chem.*, 2013, **11**, 8214–8220.

14 X. J. Feng, P. Z. Tian, Z. Xu, S. F. Chen and M. S. Wong, *J. Org. Chem.*, 2013, **78**, 11318–11325.

15 J. Pina, J. S. Seixas de Melo, R. M. F. Batista, S. P. G. Costa and M. M. M. Raposo, *J. Org. Chem.*, 2013, **78**, 11389–11395.

16 X. He, P. Zhang, J.-B. Lin, H. V. Huynh, S. E. Navarro Muñoz, C.-C. Ling and T. Baumgartner, *Org. Lett.*, 2013, **15**, 5322–5325.

17 P. Li, T. J. Sisto, E. R. Darzi and R. Jasti, *Org. Lett.*, 2014, **16**, 182–185.

18 S.-B. Ko, J.-S. Lu and S. Wang, *Org. Lett.*, 2014, **16**, 616–619.

19 S.-i. Kato, S. Shimizu, A. Kobayashi, T. Yoshihara, S. Tobita and Y. Nakamura, *J. Org. Chem.*, 2014, **79**, 618–629.

20 A. Roy, A. Datar, D. Kand, T. Saha and P. Talukdar, *Org. Biomol. Chem.*, 2014, **12**, 2143–2149.

21 T.-L. Wu, H.-H. Chou, P.-Y. Huang, C.-H. Cheng and R.-S. Liu, *J. Org. Chem.*, 2014, **79**, 267–274.

22 M. Gorecki, A. Suszczynska, M. Woznica, A. Baj, M. Wolniak, M. K. Cyranski, S. Witkowski and J. Frelek, *Org. Biomol. Chem.*, 2014, **12**, 2235–2254.

23 C. F. Gers, J. Nordmann, C. Kumru, W. Frank and T. J. J. Müller, *J. Org. Chem.*, 2014, **79**, 3296–3310.

24 F. Furche and R. Ahlrichs, *J. Chem. Phys.*, 2002, **117**, 7433–7447.

25 G. Scalmani, M. J. Frisch, B. Mennucci, J. Tomasi, R. Cammi and V. Barone, *J. Chem. Phys.*, 2006, **124**, 094107.

26 J. Liu and W. Z. Liang, *J. Chem. Phys.*, 2011, **135**, 014113.

27 J. Liu and W. Z. Liang, *J. Chem. Phys.*, 2011, **135**, 184111.

28 M. Dierksen and S. Grimme, *J. Phys. Chem. A*, 2004, **108**, 10225–10237.

29 J. Schanda, *Colorimetry: Understanding the CIE System*, Wiley, Hoboken, New Jersey, 2007.

30 F. Santoro, A. Lami, R. Improta, J. Bloino and V. Barone, *J. Chem. Phys.*, 2008, **128**, 224311.

31 J. Guthmuller, F. Zutterman and B. Champagne, *J. Chem. Theory Comput.*, 2008, **4**, 2094–2100.

32 B. Klaumuenzer, D. Kroener and P. Saalfrank, *J. Phys. Chem. B*, 2010, **114**, 10826–10834.

33 L. Goerigk and S. Grimme, *J. Chem. Phys.*, 2010, **132**, 184103.

34 R. Send, M. Kühn and F. Furche, *J. Chem. Theory Comput.*, 2011, **7**, 2376–2386.

35 E. Stendardo, F. A. Ferrer, F. Santoro and R. Improta, *J. Chem. Theory Comput.*, 2012, **8**, 4483–4493.

36 F. J. Avila Ferrer, J. Cerezo, E. Stendardo, R. Improta and F. Santoro, *J. Chem. Theory Comput.*, 2013, **9**, 2072–2082.

37 F. J. Avila Ferrer, V. Barone, C. Cappelli and F. Santoro, *J. Chem. Theory Comput.*, 2013, **9**, 3597–3611.

38 E. Bremond, M. E. Alberto, N. Russo, G. Ricci, I. Ciofini and C. Adamo, *Phys. Chem. Chem. Phys.*, 2013, **15**, 10019–10027.

39 A. Charaf-Eddin, B. Le Guennic and D. Jacquemin, *Theor. Chem. Acc.*, 2014, **133**, 1456.

40 A. D. Laurent, C. Adamo and D. Jacquemin, *Phys. Chem. Chem. Phys.*, 2014, **16**, 14334–14356.

41 K. Mitsudo, S. Shimohara, J. Mizoguchi, H. Mandai and S. Suga, *Org. Lett.*, 2012, **14**, 2702–2705.

42 C. Wetzel, A. Mishra, E. Mena-Osteritz, A. Liess, M. Stolte, F. Würthner and P. Bäuerle, *Org. Lett.*, 2014, **16**, 362–365.

43 N. Yanai, T. Mori, S. Shinamura, I. Osaka and K. Takimiya, *Org. Lett.*, 2014, **16**, 240–243.

44 S. Shinamura, E. Miyazaki and K. Takimiya, *J. Org. Chem.*, 2010, **75**, 1228–1234.

45 K. Nakanishi, T. Sasamori, K. Kuramochi, N. Tokitoh, T. Kawabata and K. Tsubaki, *J. Org. Chem.*, 2014, **79**, 2625–2631.

46 J. Tomasi, B. Mennucci and R. Cammi, *Chem. Rev.*, 2005, **105**, 2999–3094.

47 R. Cammi and B. Mennucci, *J. Chem. Phys.*, 1999, **110**, 9877–9886.

48 M. Cossi and V. Barone, *J. Chem. Phys.*, 2001, **115**, 4708–4717.

49 M. Caricato, B. Mennucci, J. Tomasi, F. Ingrosso, R. Cammi, S. Corni and G. Scalmani, *J. Chem. Phys.*, 2006, **124**, 124520.

50 R. Improta, G. Scalmani, M. J. Frisch and V. Barone, *J. Chem. Phys.*, 2007, **127**, 074504.

51 D. Jacquemin, A. Planchat, C. Adamo and B. Mennucci, *J. Chem. Theory Comput.*, 2012, **8**, 2359–2372.

52 M. J. Frisch, G. W. Trucks, H. B. Schlegel, G. E. Scuseria, M. A. Robb, J. R. Cheeseman, G. Scalmani, V. Barone, B. Mennucci, G. A. Petersson, H. Nakatsuji, M. Caricato, X. Li, H. P. Hratchian, A. F. Izmaylov, J. Bloino, G. Zheng, J. L. Sonnenberg, M. Hada, M. Ehara, K. Toyota, R. Fukuda, J. Hasegawa, M. Ishida, T. Nakajima, Y. Honda, O. Kitao, H. Nakai, T. Vreven, J. A. Montgomery, Jr., J. E. Peralta, F. Ogliaro, M. Bearpark, J. J. Heyd, E. Brothers, K. N. Kudin, V. N. Staroverov, R. Kobayashi, J. Normand, K. Raghavachari, A. Rendell, J. C. Burant, S. S. Iyengar, J. Tomasi, M. Cossi, N. Rega, J. M. Millam, M. Klene, J. E. Knox, J. B. Cross, V. Bakken, C. Adamo, J. Jaramillo, R. Gomperts, R. E. Stratmann, O. Yazyev, A. J. Austin, R. Cammi, C. Pomelli, J. W. Ochterski, R. L. Martin, K. Morokuma, V. G. Zakrzewski, G. A. Voth, P. Salvador, J. J. Dannenberg, S. Dapprich, A. D. Daniels, O. Farkas, J. B. Foresman, J. V. Ortiz, J. Cioslowski and D. J. Fox, *Gaussian 09 Revision D.01*, 2009, Gaussian Inc. Wallingford CT.

53 A. D. Laurent and D. Jacquemin, *Int. J. Quantum Chem.*, 2013, **113**, 2019–2039.

54 Y. Zhao and D. G. Truhlar, *Acc. Chem. Res.*, 2008, **41**, 157–167.

55 Y. Zhao and D. G. Truhlar, *Theor. Chem. Acc.*, 2008, **120**, 215–241.

56 F. Santoro, R. Improta, A. Lami, J. Bloino and V. Barone, *J. Chem. Phys.*, 2007, **126**, 084509.

57 F. Santoro, R. Improta, A. Lami, J. Bloino and V. Barone, *J. Chem. Phys.*, 2007, **126**, 184102.

58 This corresponds to an error of ca. 0.18 eV on the energy scale, a typical value for TD-DFT's standards (see Ref. 53 and references therein).

59 Calculation at the LR-PCM(neq)-TD-M06/6-311+G(2df,2p)//PCM-M06/6-31+G(d) level.

60 A. Charaf-Eddin, A. Planchat, B. Mennucci, C. Adamo and D. Jacquemin, *J. Chem. Theory Comput.*, 2013, **9**, 2749–2760.

61 T. Le Bahers, C. Adamo and I. Ciofini, *J. Chem. Theory Comput.*, 2011, **7**, 2498–2506.

62 D. Jacquemin, T. Le Bahers, C. Adamo and I. Ciofini, *Phys. Chem. Chem. Phys.*, 2012, **14**, 5383–5388.

Graphical Abstract

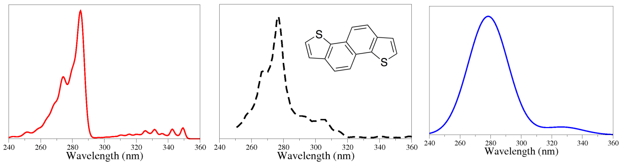

VIBRONIC EXPERIMENT VERTICAL

Vibronic effects in organic electronic building blocks.